



On-line estimation of lithium-ion battery impedance parameters using a novel varied-parameters approach

Wladislaw Waag^{a,c,*}, Christian Fleischer^{a,c}, Dirk Uwe Sauer^{a,b,c}

^a *Electrochemical Energy Conversion and Storage Systems Group, Institute for Power Electronics and Electrical Drives (ISEA), RWTH Aachen University, Germany*

^b *Institute for Power Generation and Storage Systems (PGS), E.ON ERC, RWTH Aachen University, Germany*

^c *Jülich Aachen Research Alliance, JARA-Energy, Germany*

HIGHLIGHTS

- An efficient algorithm is proposed for the estimation of battery impedance parameters.
- The battery impedance is represented as a nonlinear equivalent circuit model.
- For the first time, current dependency of battery impedance is considered by parameter estimation.
- The proposed method can be used as a basis for an adaptive prediction of the battery power.

ARTICLE INFO

Article history:

Received 17 January 2013

Received in revised form

25 February 2013

Accepted 9 March 2013

Available online 19 March 2013

Keywords:

Battery monitoring

Impedance

On-line estimation algorithm

Model parameter

ABSTRACT

In this paper a novel technique for on-line estimation of impedance parameters of a battery equivalent circuit model (ECM) is presented. The ECM is often used as a basis of battery management algorithms to calculate the state of charge or the maximal available power. Especially the latter requires that the parameters of the ECM describe precisely the battery impedance. Unfortunately, the battery impedance changes over the battery lifetime due to aging. Therefore, the parameters of the ECM must be updated continuously. In this paper such an update is achieved using a novel approach that in addition allows considering current dependency of the battery impedance. The basic idea is that the change of the battery voltage under load is predicted using the ECM with different parameter sets during a short time period. The predicted voltage is then compared to the sensor data and the best parameter set is selected. It is then used as a basis in the next adaption step. A necessary strategy for building parameter sets is implemented for a fast and efficient convergence which results in an accurate parameter estimation. The algorithm runs on a standard 16 bit 80 MHz microcontroller at only 16% processor load.

© 2013 Elsevier B.V. All rights reserved.

1. Introduction

This paper presents results of a study aiming at the development of battery monitoring algorithms for lithium-ion battery packs that are both long-term stable and self-adaptable to the state of health of the battery. Lithium-ion battery packs are always equipped with a battery management system (BMS). The BMS consists of hardware and software for battery monitoring including, among others, algorithms determining battery states. The battery states of interest

are state of charge (SoC), state of health (SoH) and some states of function (SoF), for example the prediction of a maximal available power in the next time period.

Monitoring algorithms are often based on a simplified equivalent circuit model (ECM) of the battery [1–8] or on differential equations in accordance with the equations that describe the ECM [9–12]. The ECM usually consists of a voltage source to represent the open circuit voltage (OCV) of the battery as well as of some resistances and capacitances to represent the battery's impedance characteristic. An example of such ECM is shown in Fig. 1. In many recent publications about battery management algorithms [5,6,8,11,12] the parameters of the ECM are obtained using laboratory measurements and are assumed to remain unchanged. This leads to very promising results when the ECM is used for SoC calculation or calculation of the available power of a new battery.

* Corresponding author. Institute for Power Electronics and Electrical Drives (ISEA), Jägerstrasse 17/19, D-52066 Aachen, Germany. Tel.: +49 241 8097156; fax: +49 241 8092203.

E-mail addresses: batteries@isea.rwth-aachen.de, wg@isea.rwth-aachen.de, wladislaw.waag@rwth-aachen.de (W. Waag).

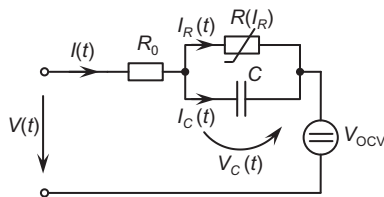


Fig. 1. Example of an equivalent circuit model (ECM) of a battery. The voltage source V_{OCV} represents the open circuit voltage (OCV) of the battery, the resistance R_0 corresponds to the internal resistance of the battery at high frequencies, the resistance $R(I_R)$ corresponds mainly to the charge transfer reaction and is current dependent (for detailed description see Section 2), the capacitance C corresponds to the double layer capacity.

However, the characteristics of the battery change significantly during its lifetime due to aging [13–18]. Then the originally measured values of impedances (resistances and capacitances) are no longer valid, which causes a high inaccuracy for battery states estimation. Especially calculation or prediction of the available power, which directly depends on the battery impedance characteristic, is not possible in this case with sufficient accuracy for aged batteries.

One of the approaches to consider changes of the battery impedance characteristic is to use joint or dual Kalman filter (KF) techniques. A Kalman filter [19] is a recursive estimator. The single Kalman filter can be used to estimate the battery SoC based on the battery ECM [5,6,8] or on any other type of battery model represented by state equations [9–12,20]. Joint and dual Kalman filters are proposed to additionally estimate parameters of the battery model [2,7,21,22]. However, this technique has some significant disadvantages:

- The basic assumption of the Kalman filter is that the measurement and model noises (inaccuracies) are described by a Gaussian probability density function. However, this assumption obviously does not relate to all applications. Although the Kalman filter is practically proven to be stable when this assumption is not exactly met, it always has a negative influence on the convergence behavior and on the accuracy of the Kalman filter [21,22].
- For consideration of nonlinearities in the battery model advanced versions of KF must be employed, such as the extended Kalman filter (EKF) or the sigma point Kalman filter (SPKF). These techniques are basically based on the substitution of non-linearity using first-order (EKF) or second-order (SPKF) Taylor series approximation. In recent publications only the nonlinearity of the SoC–OCV relation has been considered [1,2,5,9,10,12]. This is sufficient for an accurate SoC determination and can be performed with a high accuracy because the SoC of the battery changes relatively slowly, so that the linear approximation works well. However, for an accurate power calculation the significant current dependency of the battery resistance [14] as the result of the kinetics of electrode reaction [23] have to be considered additionally. In Ref. [24] it is performed using a nonlinear model in combination with EKF for lead-acid batteries. The disadvantage of this implementation is that the parameters describing the current dependency are parameterized offline for a new battery and not updated on-line. Therefore, the method would be inaccurate when it is applied for an aged battery with changed current dependency.
- The covariance of measurement and model noise has to be known a priori. An incorrect choice of them can lead to either poor convergence or too slow adaption. The adaptive extended Kalman filter (AEKF) algorithm can be used to estimate

covariance on-line [3] at the expense of an additional computing power.

- Calculations based on a Kalman filter involve matrix operations. As a result, the implementation on an ordinary low-cost microcontroller is practically difficult to achieve. Especially advanced KF techniques (EKF, AEKF, SPKF) require very high computing power. Furthermore, complex matrix operations can lead to numeric instabilities.

In Ref. [4] a simple EKF is combined with the statistical analysis of voltage pattern (SAVP) method to estimate the battery SoC and resistance. In the ECM used in that publication only the value of one resistance, called diffusion resistance, is assumed to be changing over the battery lifetime. It may be sufficient for state-of-charge and state-of-health calculations, but not for an accurate power calculation or prediction. As a further drawback the SAVP algorithm requires current and voltage profiles to be stored in the memory for a time period of over 300 s according to [4]. This limits the use of the algorithm on a low-cost microcontroller with only few kilobytes random access memory (RAM).

In Ref. [25] a passive impedance spectroscopy has been applied to monitor battery resistance. This method requires sufficient periodical current excitations at specific frequencies which may not be present in the battery load current in a particular application. This method is not suitable either for the determination of current dependency of battery resistance because of the usage of linear filters.

Another technique presented in Refs. [26–28] uses high pass filters and recursive least-square (RLS) algorithm for on-line fitting of a simple battery model to the measured data. This results in the determination of model impedances. For the consideration of the current dependency the employment of different model instances for different current ranges is proposed. The weighted outputs of each model are then added together for fitting the resulting modeled voltage to the measured battery voltage. However, it is shown that this technique works reliably only with a maximum of three current ranges, so that the current dependency is considered widely inaccurately and still vaguely [26]. Furthermore, it is not investigated how current dependency can be considered if real measured current and voltage have to be filtered by high pass filters which influences the non-linearity of these signals.

A promising approach has been presented in Refs. [29,30]. The iterative adaption of battery model parameters is performed on a basis of weighted recursive least squares (WRLS) method. There is no need for matrix operation, which makes the implementation on a low-cost microcontroller possible. However, the algorithm does not consider current dependency of model parameters.

In addition to the academic publications there is a number of patents (for example [31–33]) claiming basic ideas for the determination of the battery resistance considering the terminal current and the respective voltage change of the battery under load. Only the battery resistance as a single value can be determined using this technique. More complex impedance parameters as well as their current dependencies cannot be estimated.

As described above, the main disadvantage of the existing algorithms is that the current dependency of the battery impedance is not considered. Nevertheless, all methods show very promising results at room temperatures and for new cells because the current dependency is negligible at these conditions. However, it is substantial at lower temperatures as well as at room temperature while the battery progresses in aging. The current dependency in different states of aging is exemplarily shown in Section 2 (Fig. 2).

The disadvantages of the existing techniques provoke the need for a new method for on-line estimation of battery impedance parameters. The requirements are:

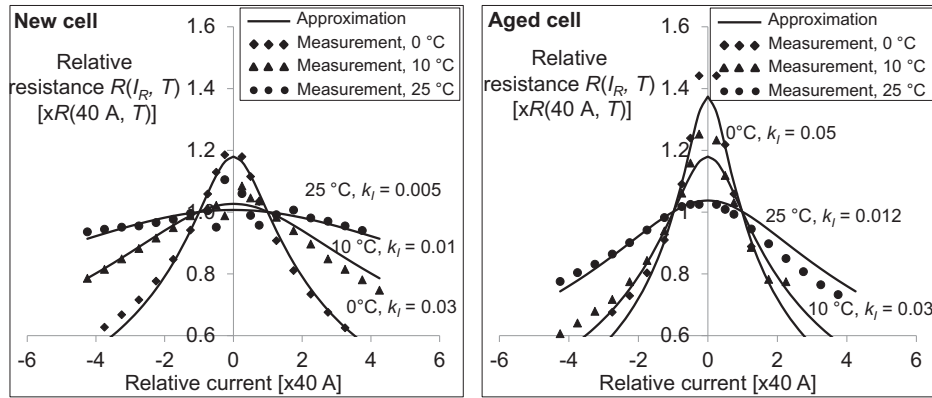


Fig. 2. Comparison between the measured and modeled (using Eq. (1)) dependency of the battery resistance on the battery current for different temperatures (40 Ah pouch cell with NMC cathode material); left: for a new cell; right: for an aged cell (after about 1900 full cycles, remaining capacity is approximately 93%).

- The ECM must be sufficient to be used as a basis for precise prediction of the available power. Especially in applications with highly-dynamic loads such as electric or hybrid vehicles, the prediction of the available power is one of the main functions of the BMS. For accurate calculation at lower temperatures the strong current dependency of the charge transfer resistance must be considered.
- The algorithm must be as simple as possible and fully adaptable to the aging of the battery as well as to various battery conditions (temperature, SoC).
- An implementation on a standard low-cost hardware must be possible, preferably at low processor load and low memory consumption.

An algorithm that meets all of these requirements is presented in the following. Section 2 describes the background and the basic idea of the method. Section 3 gives a detailed description of the algorithm. Additionally various possible improvements and variations of the algorithm are briefly introduced. In Section 4 some results are presented and discussed using an electrical vehicle as an example application. The summary in Section 5 forms the conclusion of the proposed method.

2. Background and the basic idea of the method

To fulfill the requirement regarding the possibility of power prediction, a suitable equivalent circuit battery model must be selected. We choose the model presented in Fig. 1 because it reproduces sufficiently the dynamic of the battery but is not too complex for implementation on a low-cost microcontroller. The resistance R_0 in this model corresponds to the internal resistance of the battery at high frequencies. R_0 is basically linear (current independent). The capacitance C corresponds to the double layer capacity of the battery and is also assumed to be current independent. The resistance $R(I_R)$ corresponds mainly to the charge transfer reaction. In contrast to other parameters it is highly nonlinear and can be described by the Butler–Volmer equation. Based on this equation the resistance $R(I_R)$ can be modeled as (see Appendix A):

$$R(I_R) = R_1 \cdot \left(\frac{\ln(k_I \cdot I_R + \sqrt{(k_I \cdot I_R)^2 + 1})}{k_I \cdot I_R} \right) \quad (1)$$

$R_1 [\Omega]$ is the resistance at $I_R = 0 \text{ A}$. $k_I [\text{A}^{-1}]$ is a parameter that describes the current dependency of the resistance. Both

parameters (R_1 and k_I) change for different temperatures and states of health. Fig. 2 shows exemplarily the measured and the modeled (using Eq. (1)) dependency of the relative battery resistance $R(I_R)/R(40 \text{ A})$ on the relative battery current $I/(40 \text{ A})$ for a 40 Ah lithium-ion pouch cell with nickel manganese cobalt (NMC) cathode material in a new and an aged state.

In total there are four parameters that must be adapted on-line to a given state of the battery at certain conditions (temperature, SoC, SoH): R_0 , R_1 , C and k_I . We call “parameter set (\mathbf{P})” the combination of certain values of all these parameters. For example $\mathbf{P} = \{R_0 = 1 \text{ m}\Omega, R_1 = 1 \text{ m}\Omega, C = 200 \text{ F} \text{ and } k_I = 0.01 \text{ A}^{-1}\}$.

The basic idea of the adaption algorithm is to divide the load profile on-line into short evaluation periods with duration of some 10 s each. At the beginning of each evaluation period N different parameter sets ($\mathbf{P}_1, \mathbf{P}_2, \dots, \mathbf{P}_N$) are formed and then N battery voltages at each sample step k during this period are calculated using the measured battery current and the model with these parameter sets. The voltages are then compared to the measured battery voltage. The parameter set which results in the lowest deviation between the measured and calculated voltage is selected as a basis to form parameter sets for the next evaluation period.

This is a straightforward strategy for recursive estimation. Its efficiency and accuracy depends significantly on the following two decisions:

- 1) How many different parameter sets ($\mathbf{P}_i, i = 1..N$) have to be used and how they are formed (selected).
- 2) How to select the evaluation period: when can the calculation with different parameter sets be started and when does it have to be terminated to select the best parameter set as a basis for the next evaluation period.

Before these decisions and the rest of the algorithm are described in detail in the next section, one final remark regarding the parameters R_0 , $R(I_R)$ and C will have an essential role. As mentioned earlier, these parameters correspond to certain physical effects in the battery. The proposed algorithm, as actually all adapting algorithms do, just chooses the values in a way that the modeled battery voltage fits the measured one in the best possible way. It is not guaranteed and actually not necessary that the parameters reflect exactly certain physical effects in the battery. Only the convergence to meaningful values must be ensured. This is guaranteed by using the model on the basis of physical understanding of the battery and validation tests with real new and aged battery cells.

3. Detailed algorithm description

At the beginning of this section the reference model is introduced, which is needed in the following. We call “reference model” the impedance part of the model presented in Fig. 1 with parameters from the reference parameter set $\mathbf{P}_{\text{ref}} = \{R_{0,\text{ref}}, R_{1,\text{ref}}, C_{\text{ref}}, k_{l,\text{ref}}\}$. The reference parameter set is a parameter set that is selected as a best choice during the previous evaluation period. The voltage of the reference model V_{ref} is continuously calculated at each sample step k using the reference parameter set and the measured battery current. As a part of this calculation the current $I_{C,\text{ref}}$ in the capacitance C (Fig. 1) as well as the voltage $V_{C,\text{ref}}$ are calculated. The derivation of time-discrete equations that describe the ECM is given in Appendix B.

Now the number of used parameter sets N and the strategy for their composition at the beginning of each evaluation period are selected. P is an element (R_0, R_1, C or k_l) of the parameter set \mathbf{P} . The minimal meaningful variation of each parameter P is its value P_{ref} selected as a best choice in the previous adaption period as well as a higher and a lower value, for example¹ $(1 + k_{\text{var}}) \cdot P_{\text{ref}}$ and $(1 - k_{\text{var}}) \cdot P_{\text{ref}}$ with $0 < k_{\text{var}} < 1$. In total there are $V = 3$ variations of each parameter. To consider the correlation between all $K = 4$ parameters, the full permutation of all parameters is required. It results in $N = V^K = 81$ parameter sets.

The other decision that has to be made is when to start an evaluation period and when to terminate it. Various influencing factors have to be considered:

- 2) The evaluation interval must preferably contain high current fluctuations since it increases the information content about the battery impedance in the measured battery voltage.
- 3) As shown in the following, during one single evaluation period the OCV of the battery is assumed to be constant. This is a good assumption when the evaluation period does not exceed a certain time interval (T_{max}). This maximal time interval can be adapted to a given typical load profile in the particular application.
- 4) Preferably, the next evaluation period should start directly after the previous one has been completed. Considering this, it is evident that one evaluation period should be concluded directly before the condition for starting the next estimation interval is carried out.

Based on these considerations the algorithm can be implemented as follows (Fig. 3). At the beginning, the complete algorithm is initialized (step 1). The reference parameter set \mathbf{P}_{ref} is selected. It can be the initial parameter set for a new cell or the latest calculated parameter set stored in the non-volatile memory of the BMS. In addition the reference model is initialized: $I_{C,\text{ref}} = 0$, $V_{C,\text{ref}} = 0$.

Every time a new measured battery voltage and current ($V(k)$ and $I(k)$) values are available (at each sample step k), the following calculations are performed:

-The reference model is calculated (step 3):

$$R_{\text{ref}}(I_R(k)) = R_{1,\text{ref}} \cdot \left(\frac{\ln \left(k_{l,\text{ref}} \cdot (I(k) - I_C(k-1)) + \sqrt{(k_{l,\text{ref}} \cdot (I(k) - I_C(k-1)))^2 + 1} \right)}{k_{l,\text{ref}} \cdot (I(k) - I_C(k-1))} \right) \quad (2)$$

$$V_{C,\text{ref}}(k) = \frac{V_{C,\text{ref}}(k-1) \cdot (2 \cdot R_{\text{ref}}(I_R(k)) \cdot C_{\text{ref}} / \Delta t - 1) + R_{\text{ref}}(I_R(k)) \cdot (I(k) + I(k-1))}{2 \cdot R_{\text{ref}}(I_R(k)) \cdot C_{\text{ref}} / \Delta t + 1} \quad (3)$$

- 1) The calculation of the model voltage cannot be started without knowing the previous voltage V_C of the capacitance C , since it depends on the previous history. To minimize the influence of the previous history on the voltage calculation during the present evaluation period, the calculation must be preferably started when current I_C through the capacitance C is low over a short time interval because the voltage V_C is mainly defined by the resistance $R(I_R)$ in this case and depends less from previous history. The continuously calculated reference model as described above can be used for that. As soon as $I_{C,\text{ref}}$ stays in a certain range ($|I_{C,\text{ref}}| < I_{C,\text{max}}$) over a short time interval (Δt_{IC}), the evaluation period can be started and the model for each parameter set can be initialized with $V_{C,\text{ref}}$. The current I_C is low when the dynamic of the total battery current I is low at a given time, which does practically often happen in many applications. Both algorithm parameters ($I_{C,\text{max}}$ and Δt_{IC}) must be selected appropriately for a particular application as exemplarily discussed in Section 4.

$$I_{C,\text{ref}}(k) = I(k) - V_{C,\text{ref}}(k) / R_{\text{ref}}(I_R(k)) \quad (4)$$

$$V_{\text{ref}}(k) = V_{C,\text{ref}}(k) + I(k) \cdot R_{0,\text{ref}} \quad (5)$$

$\mathbf{P}_{\text{ref}} = \{R_{0,\text{ref}}, R_{1,\text{ref}}, C_{\text{ref}}, k_{l,\text{ref}}\}$ is a reference parameter set, $\Delta t = t(k) - t(k-1)$ is a sample time period.

-If the evaluation period is presently inactive, the condition for the start of a new evaluation period is checked (step 5). As described above, this condition is that $I_{C,\text{ref}}$ is accordingly low ($|I_{C,\text{ref}}| < I_{C,\text{max}}$) over a short time interval (Δt_{IC}). If this is the case, then $N = 81$ new parameter sets are computed using \mathbf{P}_{ref} as a basis (step 6). The battery model is initialized for each parameter set $\mathbf{P}_i = \{R_{0,i}, R_{1,i}, C_i, k_{l,i}\}$, $i = 1..N$ (step 7):

$$V_{C,i}(k) = V_{C,\text{ref}}(k) \quad \text{and} \quad V_i(k) = V(k) \quad (6)$$

$$V_{OCV,i} = V(k) - V_{C,i}(k) - I(k) \cdot R_{0,i} \quad (7)$$

In addition the accumulated quadratic deviation $Q_i(k)$ between the measured battery voltage and the modeled battery voltage for each parameter set is reset to zero:

$$Q_i(k) = (V(k) - V_i(k))^2 = 0 \quad (8)$$

Consequently the new evaluation period is marked as being active.

¹ As an alternative, the variation of the parameter P can be defined as $\{k_{\text{var}} \cdot P_{\text{ref}}, 1/k_{\text{var}} \cdot P_{\text{ref}}\}$ with $0 < k_{\text{var}} < 1$. However, it requires a division operation that is inefficient on a low-cost microcontroller without floating-point unit.

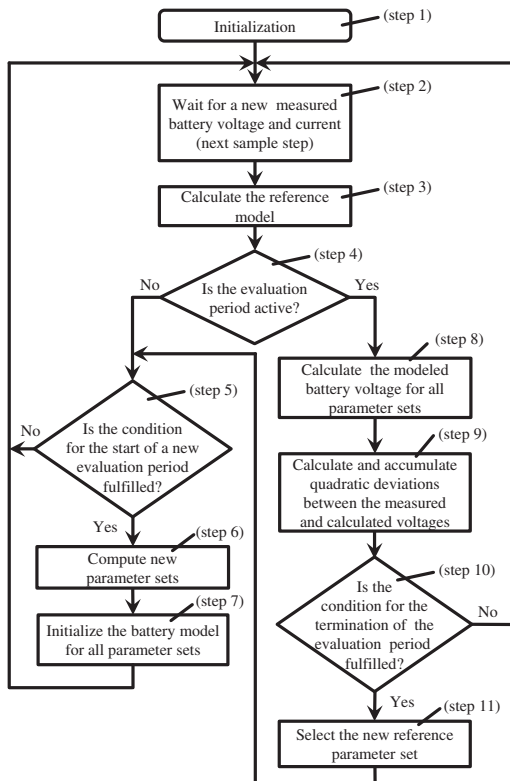


Fig. 3. Algorithm for the determination of impedance parameters of the battery equivalent circuit model.

-If the evaluation period is presently active, the battery model is calculated for all parameter sets \mathbf{P}_i first (step 8):

$$R_i(I_R(k)) = R_{1,i} \cdot \left(\frac{\ln \left(k_{I,i} \cdot (I(k) - I_{C,i}(k-1)) + \sqrt{(k_{I,i} \cdot (I(k) - I_{C,i}(k-1)))^2 + 1} \right)}{k_{I,i} \cdot (I(k) - I_{C,i}(k-1))} \right) \quad (9)$$

$$V_{C,i}(k) = \frac{V_{C,i}(k-1) \cdot (2 \cdot R_i(I_R(k)) \cdot C_i / \Delta t - 1) + R_i(I_R(k)) \cdot (I(k) + I(k-1))}{(2 \cdot R_i(I_R(k)) \cdot C_i / \Delta t + 1)} \quad (10)$$

$$I_{C,i}(k) = I(k) - V_{C,i}(k) / R_i(I_R(k)) \quad (11)$$

$$V_i(k) = V_{OCV,i} + V_{C,i}(k) + I(k) \cdot R_{0,i} \quad (12)$$

The accumulated quadratic deviation $Q_i(k)$ between the measured battery voltage and the modeled battery voltage is updated for each parameter set (step 9):

$$Q_i(k) = Q_i(k-1) + (V(k) - V_i(k))^2 \quad (13)$$

Now the condition for the termination of the present evaluation period is examined (step 10). It is fulfilled, if at least one of two prerequisites is satisfied:

- 1) The condition for a start of a new evaluation period is fulfilled ($I_{C,ref}$ is small as described above) and there is enough current

change in the active evaluation period ($I_{max} - I_{min} > \Delta I_{min}$). For the evaluation of the latest condition the minimum and maximum measured battery currents (I_{min}, I_{max}) are recorded during each evaluation period. In this case after the termination of the present evaluation period the next evaluation is initialized immediately.

- 2) The duration of an active evaluation period is too long, so that the initially assumed OCV of the battery has most likely changed significantly. This is a necessary condition because according to Eq. (12) the OCV is assumed to be constant during each evaluation period. For the evaluation of this condition the battery current can be integrated for each evaluation period. This integral must be lower than a certain predefined value (q_{max}) that causes high OCV change.²

If the active evaluation period is terminated, all calculated quadratic deviations are compared and the one with the lowest value is selected: $Q_{ref} = \min(Q_i), i = 1..N$ (step 11). The respective parameter set is then selected as the new present reference set: $\mathbf{P}_{ref} = \mathbf{P}(Q_{ref})$. Consequently the present evaluation period is marked as being inactive and the next period can be initiated after checking the conditions in step 5.

3.1. Further improvements and variations of the algorithm

The main idea of the proposed algorithm is relatively simple compared to existing methods (e.g. Kalman filter) proposed in literature. Only direct model calculations are used which allow easily different variations and improvements. Some of them will only be addressed briefly in the following because more detailed examination would be beyond the scope of this paper. The intention here is to give the reader some ideas how to adapt the proposed algorithm for needs in a particular application.

- 1) The variation of each parameter P is controlled by the coefficient k_{var} : $P_{1..3} = \{(1 - k_{var}) \cdot P_{ref}, P_{ref}, (1 + k_{var}) \cdot P_{ref}\}$ to generate new parameter sets. This coefficient can be selected to be constant or adaptive at the beginning of each evaluation period. For example its value can be set higher by the initialization of the algorithm because the likelihood for an inaccurate initialization of the reference parameter set is high. During adaption its value can then be decreased consequently when the calculated quadratic deviation Q between the measured and calculated battery voltage is decreasing. However, the minimal value must be higher than zero because the algorithm still has to

² In fact the battery OCV calculated according to Eq. (7) may additionally include other overvoltages caused by the battery previous history (previous current flow). These overvoltages can also change during the evaluation period and influence the results. Therefore the duration of the evaluation period must be additionally limited.

track changes of the battery impedance caused by changing conditions (SoC, temperature) during battery operation.

- 2) The strategy for generating parameter sets can be chosen completely different. For example, methods derived from genetic algorithm or simplex algorithm can be applied.
- 3) When the temperature of the battery changes very fast, then relatively fast adaption must be used with a high adaption coefficient k_{var} . However, this will lead to noisy parameter values. When the basic temperature dependency of the battery impedance parameters is known, this information can be utilized instead of increasing the adaption coefficient k_{var} . For this the reference parameter set is additionally updated depending on the temperature change between two evaluation periods. The simple assumption of the doubling of battery resistances (R_0 and R_1) with each 10 K temperature increase (in accordance to Arrhenius law) can already improve the accuracy of the algorithm significantly by fast temperature changes. In the case that a greater accuracy of temperature dependency is known for a given cell, it can be used instead. The same technique can also be applied for an additional correction by fast SoC changes if the basic dependency of parameters on SoC is known.
- 4) When the dependency of the battery's OCV on SoC is known and the SoC is determined by any other algorithm, a compensation of OCV change can be performed during each evaluation period. An additional term can be integrated into Eq. (12):

$$V_i(k) = V_{OCV,i} + V_{C,i}(k) + I(k) \cdot R_{0,i} + \nu(\text{SoC}) \cdot \sum_{\text{eval.period}} I(k) \cdot \Delta t \quad (14)$$

$\nu(\text{SoC})$ is the change of battery OCV per 1 As current flow [$\text{V A}^{-1} \text{s}^{-1}$].

- 5) In step 11 instead of the direct definition of a new reference parameter set the previous history of parameter changes can be considered by employing low pass filtering. The new parameters P of the reference parameter set are defined as $P_{\text{ref,new}} = k_{LP} \cdot P_{\text{ref,old}} + (1 - k_{LP}) \cdot P_{\text{ref,Qmin}}$ with $0 < k_{LP} < 1$. The advantage is that the inaccuracy of the parameter estimation in each evaluation period is compensated by filtering and the resulting parameters are less noisy.
- 6) As shown in Fig. 2 the modeling of the current dependency of the resistance $R(I_R)$ by Eq. (1) is not very accurate. The results of applying the proposed adaption algorithm can be adjusted to be more accurate for higher or lower current rates depending on the requirements in the particular application. For this, an additional weighting factor $W(I(k))$ can be employed through calculation of the quadratic deviation between measured and modeled battery voltage (Eq. (12)):

$$Q_i(k) = Q_i(k-1) + W(I(k)) \cdot (V_i(k) - V(k))^2 \quad (15)$$

If this weighting factor $W(I)$ is higher for higher current rates, the model parameters will be adapted to reproduce the battery voltage more accurately at higher currents than at lower currents. Other strategies are also possible.

- 7) The application of the adaption algorithm is not limited to the proposed battery model. It is possible to use alternative equivalent battery circuit models.

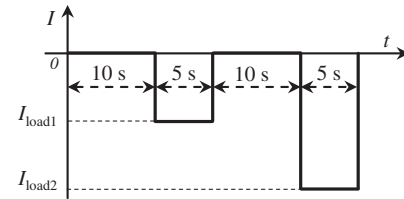


Fig. 4. Current pattern periodically integrated into real load profile for verification tests.

4. Verification using an electrical vehicle as an example application

As mentioned in the introduction, the exact estimation of battery impedance parameters is especially required for accurate prediction of the available power. This function of the BMS is of particular importance in electric vehicles with lithium-ion battery packs. Therefore, this application is most suitable to verify the proposed algorithm.

The available power is limited by the maximum current that can be applied to the battery so that the battery voltage does not exceed predefined voltage limits. It must be ensured because of safety reasons. The core of each power prediction algorithm is the prediction of the battery voltage for a certain load current I_{load} . The more accurate the prediction of the voltage, the higher is the accuracy of the power prediction. Therefore, to qualify the accuracy of the proposed algorithm, it is meaningful to use estimated impedance parameters for the prediction of the battery voltage and to compare this predicted voltage to the voltage measured by the test bench.

As a basis for verification tests a battery load profile measured in an electric vehicle prototype during city driving is used. The current

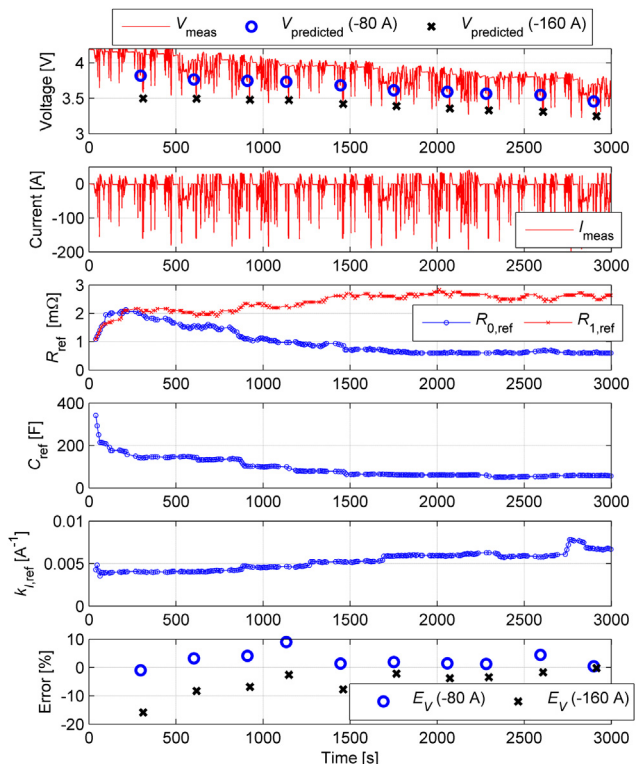


Fig. 5. Result of applying the proposed algorithm on a new 40 Ah lithium-ion cell. The voltage error (E_V) is calculated according to Eq. (16).

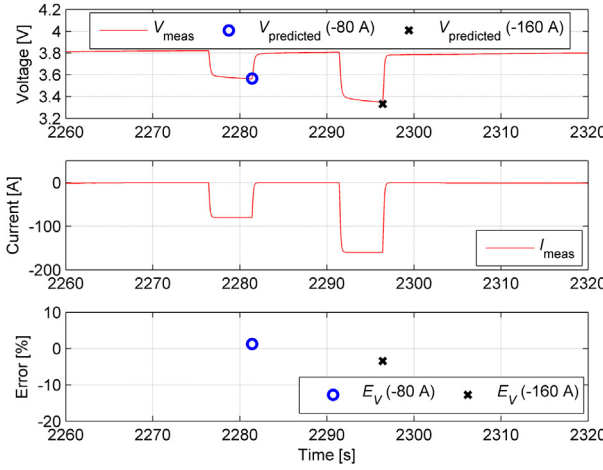


Fig. 6. Detailed representation of one of the artificial test current patterns (at $t = 2260$ s) in Fig. 5.

pattern shown in Fig. 4 is periodically integrated into this profile approximately after each 5 min to have deterministic points for the verification of voltage prediction. This current pattern consists of two current pulses with different currents $I_{\text{load}1} = -80$ A and $I_{\text{load}2} = -160$ A. The resulting current profile is then applied to the battery cell using a battery test bench system manufactured by the company Digatron. The battery cell under test is placed in a temperature chamber.

At the beginning of each current pulse the cell voltage at the end of the pulse is predicted ($V_{\text{predicted}}$) and then compared to the measured voltage (V_{meas}). The relative voltage error is used as a prediction inaccuracy:

$$E_V = \Delta V / V_{\text{drop}} = (V_{\text{predicted}} - V_{\text{meas}}) / V_{\text{drop}} \quad (16)$$

$V_{\text{drop}} = (V_{\text{meas, start}} - V_{\text{meas, end}})$ is the difference between voltage measured directly before the current pulse and the voltage measured at the end of the current pulse.

The above definition of prediction inaccuracy is useful because it reflects the inaccuracy of the determination of the total battery resistance ($R_0 + R(I_R)$). Furthermore, it gives a very good approximation for the inaccuracy of power prediction that can be implemented based on this method. It should be noted that this definition differs significantly from often used definition related to the total battery voltage ($E_V = \Delta V / V_{\text{meas}}$) and leads to higher error values, but is more adequate.

The voltage prediction is performed using the model shown in Fig. 1 and the reference parameter set \mathbf{P}_{ref} that is valid at each given time:

$$V_{\text{predicted}} = V_{t=0} + I_{\text{load}} \cdot R_{0,\text{ref}} + I_{\text{load}} \cdot R(I_{\text{load}}) \cdot \left(1 - \exp \left(\frac{-T_{\text{pulse}}}{R(I_{\text{load}}) \cdot C_{\text{ref}}} \right) \right) \quad (17)$$

$V_{t=0}$ is the battery voltage measured directly before the beginning of the respective current pulse. $T_{\text{pulse}} = 5$ s is the duration of the current pulse.

Firstly a new 40 Ah lithium-ion cell with NMC cathode material is used for the verification tests. The result is shown in Fig. 5. The battery was fully charged and the temperature is controlled at 0 °C before starting the test. The initial parameters of the battery model

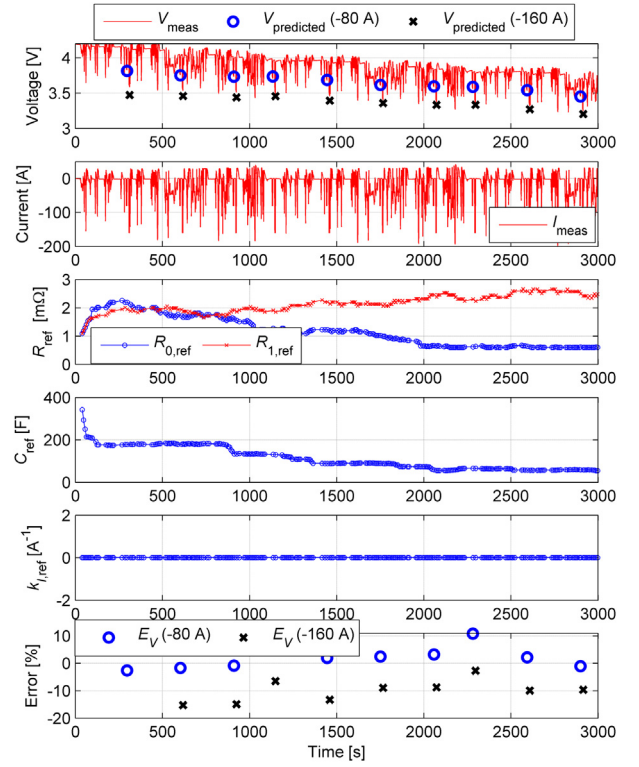


Fig. 7. Results of applying the proposed algorithm on a new 40 Ah lithium-ion cell with current dependency switched off (k_i is fixed to zero). The voltage error (E_V) is calculated according to Eq. (16).

were intentionally selected very unsuitable for the cell under the given conditions to show the adaption ability of the algorithm. Within the first 250 s the values of R_0 , R_1 and C are significantly adapted so that the prediction of the battery voltage is possible even though the inaccuracy at high discharge current is still very high. The adaption of the parameter k_i as well as the respective correction of R_0 , R_1 and C takes a longer time because the current dependency can be sufficiently “learned” only at high currents, but the share of high currents in this load profile is rather small.³ At the end of the test profile the prediction of the battery voltage at high currents is as accurate as at low currents. Fig. 6 shows detailed zoom of one of the last current patterns in Fig. 5. It can be clearly seen that the predicted voltage describes very accurately the voltage drop caused by the current pulse.

To emphasize the importance of the consideration of current dependency of the battery impedance, the same profile is used again with the proposed algorithm, but with the current de-

pendency switched off (k_i is fixed to zero). The results are presented in Fig. 7. As can be seen, the prediction of the battery voltage is significantly more inaccurate in this case.

³ In this example the battery current exceeds ± 40 A in only 23% of time and exceeds ± 80 A in only 9.3% of time.

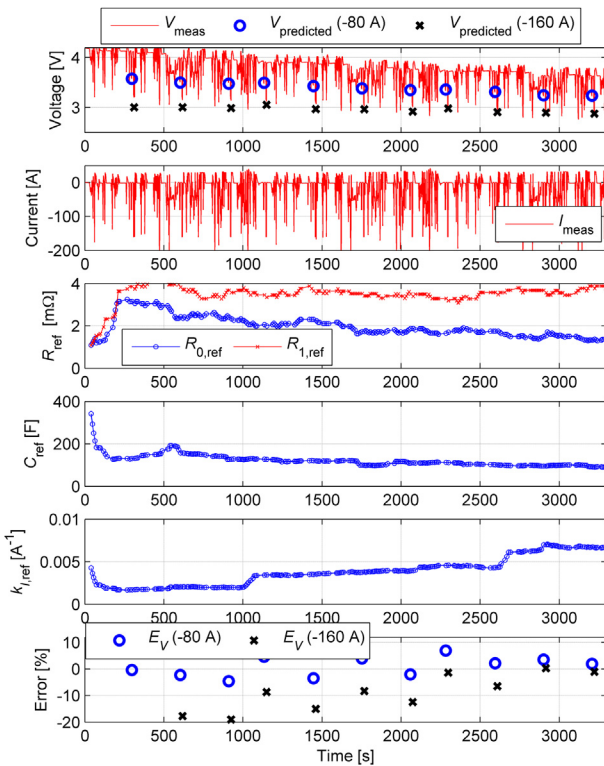


Fig. 8. Results of applying the proposed algorithm on an aged 40 Ah lithium-ion cell. The voltage error (E_V) is calculated according to Eq. (16).

Fig. 8 shows results when the proposed algorithm is applied to the same battery as in **Fig. 5**, however, the state of health is lower (aging is advanced). The battery was fully charged and the

Table 1
Parameters of the algorithm.

Parameter	Value	Recommendation for the selection
k_{var}	0.05	This parameter controls the variation of single model parameters in parameter sets. Higher values lead to faster parameter adaption but cause noisy outputs. Values between 0.03 and 0.1 seem to be a good first choice.
k_{LP}	0.3	This parameter influences the relation between the adaption speed and the output noise of the model parameters. Higher values lead to slower adaption but less noisy outputs. Values between 0.1 and 0.5 seem to be a good first choice.
$I_{\text{C,max}}$	10 A	This parameter controls if a new evaluation period can be started. Its selection depends on the dynamic of the load current. For the considered electric vehicle application the values in the range of 5%–20% of the maximal battery load current is a good choice.
Δt_{IC}	0.3 s	This parameter controls if new evaluation period can be started. It must be 3–5 times higher than the used sample time Δt .
T_{max}	30 s	This parameter defines the maximum duration of each evaluation period. It must be defined in a way that sufficient fluctuations of the battery load current occur in this time period. For the considered electric vehicle application a good range is 10–40 s.
ΔI_{min}	10 A	This parameter defines the current fluctuation that is sufficient for observation of the battery impedance in the measured battery voltage. It must be chosen significantly higher than the inaccuracy of the current measurement hardware but preferably lower than the typical RMS value of the load current.

temperature is controlled at 10 °C before starting the test. The initial model parameters were set to the same values as in the test using the new cell (**Fig. 5**). The adaption takes slightly longer time to reach the same accuracy as for the new cell. However, in a real application the parameters are adapted continuously so that each time the algorithm is initialized with very good starting parameters. Therefore the adaption rate achieved by the proposed algorithm is absolutely sufficient.

The parameters of the algorithm described in Section 3 and used by verification tests are summarized in **Table 1**. The selection of these parameters depends rather on the application and on typical load profiles than on the battery properties. All parameters can be freely selected in a certain meaningful range. They can also be further optimized considering particular applications by performing several verification tests as long as a statistically sufficient number of battery load profiles in this application are available.

5. Conclusion

The presented algorithm shows very promising results for battery impedance parameters determination and for prediction of battery voltage. Therefore, it can be used as a core algorithm for the prediction of the maximal available power of the battery. In our future work we are going to develop such an algorithm including consideration of the variation between parameters of single cells in a lithium-ion battery pack.

The main advantage and the novelty of the proposed algorithm is the strong consideration of the current dependency of the battery resistance which is substantial at lower temperatures. Furthermore, the algorithm is fully self-adaptable to the aging state of the battery as well as to the battery conditions (temperature, SoC).

The question of stability and correct convergence at all possible conditions has not been investigated systematically in this work. However, the algorithm is very likely to fulfill these requirements. The reason is that in contrast to other recursive algorithms the parameters of the battery model are not updated in each sample step. The battery is observed over an evaluation period (typically 10–20 s in the considered application) and parameters are updated only when substantial information is gathered. This approach prevents parameters to be updated in an incorrect direction and suppresses possible convergence problems.

The proposed model reproduces the behavior of the battery well during short time periods. If voltage prediction has to be performed for significantly longer time periods, the additional consideration of other processes in the battery (diffusion, change of the battery open circuit voltage under load) will be required to keep high accuracy.

The algorithm has been implemented on a low-cost 16 bit microcontroller operated at 80 MHz (Infineon XC2287 [34]). Floating point operations are emulated because the microcontroller does not provide a floating-point unit. The consumption of RAM is 1520 Byte (1.8%), the consumption of ROM (read-only memory) is about 14 kByte (1.8%) and the average processor load is about 16% at 10 Hz sample rate. These characteristics are achieved in spite of the need to calculate the model $N = 81$ times in parallel with $N = 81$ different parameter sets. The reason is that the used equations (Eq. (10)–(12)) contain only one time consuming division operation when the sample rate is taken constant. Multiplications and additions are performed very fast even though the microcontroller does not provide a floating-point unit. The calculation of the function for the current dependency of the battery resistance in Eq. (9) in the form $\ln(x + \sqrt{x^2 + 1})/x$ is implemented as look-up table. Further optimization in fixed-point is possible.

Appendix A. Modeling the current dependency of battery resistance $R(I_R)$

The resistance $R(I_R)$ corresponds mainly to the charge transfer reaction, that can be described by the Butler–Volmer equation:

$$I_R = A \cdot i_0 \cdot \left(\exp\left(\frac{a_a \cdot n \cdot F}{R_g \cdot T} \cdot V_C\right) - \exp\left(\frac{-a_c \cdot n \cdot F}{R_g \cdot T} \cdot V_C\right) \right) \quad (\text{A.1})$$

A is the electrode active surface area; a_c and a_a are cathodic and anodic charge transfer coefficients ($a_c + a_a = 1$; $a_c, a_a > 0$); n is the number of electrons involved in the electrode reaction; F is the Faraday constant; R_g is the universal gas constant; T is an absolute temperature; V_C is the activation overpotential.

Assuming the cathodic and anodic charge transfer reaction coefficients to be equal ($a_c = a_a$) (which is quite correct for lithium-ion batteries) as well as using substitutions $I_0 = 2 \cdot A \cdot i_0$ and $K = \frac{a_a \cdot n \cdot F}{R_g \cdot T}$, the Butler–Volmer equation can be denoted as:

$$I_R = I_0 \cdot \left(\frac{\exp(K \cdot V_C) - \exp(-K \cdot V_C)}{2} \right) \quad (\text{A.2})$$

Applying the definition of the hyperbolic sine function $y = \sinh(x) = (\exp(x) - \exp(-x))/2$ and using its inverse $x = \sinh^{-1}(y)$, the activation overpotential can be expressed as [35,36]:

$$V_C = \frac{1}{K} \cdot \sinh^{-1}\left(\frac{I_R}{I_0}\right) \quad (\text{A.3})$$

The resistance $R(I_R)$ is then defined as:

$$R(I_R) = \frac{V_C}{I_R} = \frac{1}{K \cdot I_R} \cdot \sinh^{-1}\left(\frac{I_R}{I_0}\right) \quad (\text{A.4})$$

Finally, using substitutions $R_1 = (I_0 \cdot K)^{-1}$ and $k_I = 1/I_0$ as well as the definition of the inverse hyperbolic sine function as logarithm $\sinh^{-1}(x) = \ln(x + \sqrt{x^2 + 1})$, the resistance can be expressed as:

$$V_C(z) = \frac{z^{-1} \cdot V_C(z) \cdot (2 \cdot R(I_R(z)) \cdot C/\Delta t - 1) + R(I_R(z)) \cdot (I(z) + z^{-1} \cdot I(z))}{2 \cdot R(I_R(z)) \cdot C/\Delta t + 1} \quad (\text{B.8})$$

$$R(I_R) = R_1 \cdot \left(\frac{\ln\left(k_I \cdot I_R + \sqrt{(k_I \cdot I_R)^2 + 1}\right)}{k_I \cdot I_R} \right) \quad (\text{A.5})$$

The singularity at $I_R = 0$ can be avoided by substitution of this equation with

$$R(I_R = 0) = \lim_{I_R \rightarrow 0} R_1 \cdot \left(\frac{\ln\left(k_I \cdot I_R + \sqrt{(k_I \cdot I_R)^2 + 1}\right)}{k_I \cdot I_R} \right) = R_1 \quad (\text{A.6})$$

Appendix B. Derivation of time-discrete model equations

The model shown in Fig. 1 can be described in time domain by the following equations based on the Kirchhoff's circuit laws:

$$V(t) = V_{\text{OCV}}(t) + V_C(t) + I(t) \cdot R_0 \quad (\text{B.1})$$

$$R(I_R(t)) = R_1 \cdot \left(\frac{\ln\left(k_I \cdot I_R(t) + \sqrt{(k_I \cdot I_R(t))^2 + 1}\right)}{k_I \cdot I_R(t)} \right) \quad (\text{B.2})$$

$$V_C(t) = \left(I(t) - C \cdot \frac{dV_C(t)}{dt} \right) \cdot R(I_R(t)) \quad (\text{B.3})$$

Eq. (B.1) and Eq. (B.2) can be directly transformed into time-discrete domain:

$$V(k) = V_{\text{OCV}}(k) + V_C(k) + I(k) \cdot R_0 \quad (\text{B.4})$$

$$R(I_R(k)) = R_1 \cdot \left(\frac{\ln\left(k_I \cdot I_R(k) + \sqrt{(k_I \cdot I_R(k))^2 + 1}\right)}{k_I \cdot I_R(k)} \right) \quad (\text{B.5})$$

Eq. (B.3) can be transformed using Laplace-Transformation first:

$$V_C(s) = (I(s) - s \cdot C \cdot V_C(s)) \cdot R(I_R(s)) \quad (\text{B.6})$$

Applying the bilinear transformation:

$$s = \frac{2}{\Delta t} \cdot \frac{1 - z^{-1}}{1 + z^{-1}} \quad (\text{B.7})$$

and after some simple transformations the following time-discrete equation can be obtained:

Finally it can be denoted using time step index k :

$$V_C(k) = \frac{V_C(k-1) \cdot (2 \cdot R(I_R(k)) \cdot C/\Delta t - 1) + R(I_R(k)) \cdot (I(k) + I(k-1))}{2 \cdot R(I_R(k)) \cdot C/\Delta t + 1} \quad (\text{B.9})$$

The direct calculation of $V_C(k)$ according to this equation is not possible because it contains the dependency on $R(I_R(k))$ that depends on $V_C(k)$. However, to avoid the need of the recursive calculation each time step k , the current used by the calculation of the resistance $R(I_R(k))$ can be approximated by

$$I_R(k) = I(k) - I_C(k) \approx I(k) - I_C(k-1) \quad (\text{B.10})$$

It results in

$$R(I_R(k)) = R_1 \cdot \left(\frac{\ln\left(k_I \cdot (I(k) - I_C(k-1)) + \sqrt{(k_I \cdot (I(k) - I_C(k-1)))^2 + 1}\right)}{k_I \cdot (I(k) - I_C(k-1))} \right) \quad (\text{B.11})$$

This approximation is possible without causing convergence problems because the current I_C in the capacitance changes slowly. At steady state conditions the simplification does not cause any error.

References

- [1] C. Hu, B.D. Youn, J. Chung, Applied Energy 92 (2012) 694–704.
- [2] X.-s. Hu, F.-c. Sun, X.-m. Cheng, Journal of Zhejiang University – Science A 12 (2011) 818–825.
- [3] H. He, R. Xiong, H. Guo, Applied Energy 89 (2012) 413–420.
- [4] J. Kim, B.H. Cho, Vehicular Technology, IEEE Transactions on 60 (2011) 4249–4260.
- [5] J. Lee, O. Nam, B.H. Cho, Journal of Power Sources 174 (2007) 9–15.
- [6] J. Li, B. Jia, M. Mazzola, M. Xin, On-line battery state of charge estimation using Gauss-Hermite quadrature filter, in: Proceedings of Applied Power Electronics Conference and Exposition (APEC), 2012, pp. 434–438.
- [7] M. Urbain, S. Rael, B. Davat, P. Desprez, State Estimation of a Lithium-Ion Battery through Kalman Filter, in: IEEE Power Electronics Specialists Conference, PESC 2007, 2007, pp. 2804–2810.
- [8] K.X. Wei, Q.Y. Chen, Advanced Materials Research 403–408 (2011) 2211–2215.
- [9] G.L. Plett, Journal of Power Sources 134 (2004) 262–276.
- [10] G.L. Plett, Journal of Power Sources 161 (2006) 1356–1368.
- [11] K.W.E. Cheng, B.P. Divakar, H. Wu, K. Ding, H.F. Ho, Vehicular Technology, IEEE Transactions on 60 (2011) 76–88.
- [12] F. Sun, X. Hu, Y. Zou, S. Li, Energy 36 (2011) 3531–3540.
- [13] M. Ecker, J.B. Gerschler, J. Vogel, S. Käbitz, F. Hust, P. Dechent, D.U. Sauer, Journal of Power Sources 215 (2012) 248–257.
- [14] W. Waag, S. Käbitz, D.U. Sauer, Applied Energy 102 (2013) 885–897.
- [15] M. Broussely, P. Biensan, F. Bonhomme, P. Blanchard, S. Herreyre, K. Nechev, R.J. Staniewicz, Journal of Power Sources 146 (2005) 90–96.
- [16] D.P. Abraham, J.L. Knuth, D.W. Dees, I. Bloom, J.P. Christophersen, Journal of Power Sources 170 (2007) 465–475.
- [17] M. Safari, C. Delacourt, Journal of The Electrochemical Society 158 (2011) A1123–A1135.
- [18] R.G. Jungst, G. Nagasubramanian, H.L. Case, B.Y. Liaw, A. Urbina, T.L. Paez, D.H. Doughty, Journal of Power Sources 119–121 (2003) 870–873.
- [19] S. Haykin, Kalman Filtering and Neural Networks, John Wiley & Sons, Inc., 2001.
- [20] G.L. Plett, Journal of Power Sources 134 (2004) 252–261.
- [21] G.L. Plett, Journal of Power Sources 134 (2004) 277–292.
- [22] G.L. Plett, Journal of Power Sources 161 (2006) 1369–1384.
- [23] A.J. Bard, G. Inzelt, F. Scholz, Electrochemical Dictionary, Springer-Verlag, 2008.
- [24] L.W. Juang, P.J. Kollmeyer, T.M. Jahns, R.D. Lorenz, Improved nonlinear model for electrode voltage-current relationship for more consistent online battery system identification, in: Proceedings of IEEE Energy Conversion Congress and Exposition (ECCE), 2011, pp. 2628–2634.
- [25] O. Bohlen, Impedance-Based Battery Monitoring, RWTH Aachen University, Ph.D. thesis, 2008.
- [26] M.A. Roscher, Zustandserkennung von LiFePO4-Batterien für Hybrid-und Elektrofahrzeuge, RWTH Aachen University, Ph.D. thesis, 2010.
- [27] M. Roscher, Verfahren zur Bestimmung und/oder Vorhersage der Hochstrombelastbarkeit einer Batterie, DE 102009049320 A1, 2011.
- [28] M.A. Roscher, O.S. Bohlen, D.U. Sauer, Energy Conversion, IEEE Transactions on 26 (2011) 737–743.
- [29] M. Verbrugge, Journal of Applied Electrochemistry 37 (2007) 605–616.
- [30] S. Wang, M. Verbrugge, J.S. Wang, P. Liu, Journal of Power Sources 196 (2011) 8735–8741.
- [31] S. Uperty and E. McKernan, System and Method to Determine an Internal Resistance and State of Charge, State of Health, or Energy Level of a Rechargeable Battery, US 2011/0172939 A1, 2011.
- [32] H. Singh, T.G. Palanisamy, R.B. Huykman, W.C. Hovey, System and Method for Determining Battery State-of-Health, US 6469512, 2002.
- [33] E. Barsukov, D.R. Poole, D.L. Freeman, Battery Internal Impedance Determining Method, Involves Computing Internal Impedance By Dividing Difference Between Battery Voltage and Open Circuit Voltage at Present Depth of Discharge By Average Steady Current Value, US 6832171, 2004.
- [34] Infineon Technologies AG, (visited in Mai 2012) Products (Online), <http://www.infineon.com>
- [35] P.J. Gellings, H.J.M. Bouwmeester, The CRC Handbook of Solid State Electrochemistry, CRC Press, 1997.
- [36] D.A. Noren, M.A. Hoffman, Journal of Power Sources 152 (2005) 175–181.